Neutron scattering study on decomposition in Cu-Ni-Fe alloys

J. Aalders and C. van Dijk
Netherlands Energy Research Foundation ECN, P.O. Box 1, 1755 ZG Petten, The Netherlands

S. Radelaar
Laboratory of Metallurgy, Delft University of Technology, Rotterdamseweg 137, 2628 AL Delft, The Netherlands

(Received 30 November 1983)

The validity of current theories for describing decomposition was investigated for a number of Cu-Ni-Fe alloys by means of neutron scattering. The dynamical scaling procedure of the structure function during decomposition was successful only in some particular cases of decomposition. As a measure for the size of the nuclei that are formed during decomposition of an alloy, we considered the radius of gyration and the first and second moment of the scattering function. The coarsening of the alloys could, except for the later stages, be described by the Lifshitz-Slyozov theory. Superlattice reflections were found in the diffraction pattern of $Cu_{52}Ni_{38}Fe_{10}$ after annealing for 665 and 857 h at 733 K. We attribute this to the formation of an ordered Ni_3Fe-type structure.

I. INTRODUCTION

The concept of separating the miscibility gap into a thermodynamically metastable and unstable region was first introduced by Gibbs.[1] According to the early theories there is an energy barrier to decomposition in the metastable regime and the alloy will decompose by the mechanism of nucleation and growth. Small nuclei of the new phase will form upon prolonged annealing. Accordingly, in the metastable regime there is an instability with respect to local perturbations that are large in degree (large composition difference with the surrounding matrix) but small in extent (small nuclei). In the unstable regime there is an instability with respect to nonlocal perturbations (spinodal decomposition) that are small in degree (small composition difference with the surrounding matrix) but large in extent (long-wavelength composition fluctuations).

Distinguishing, experimentally, between the mechanism of spinodal decomposition and nucleation and growth turned out to be very difficult. Gibbs assumed that the spinodal line, which separates the metastable from the unstable regime, is a sharp boundary. However, experimental results,[2,3] more elaborate theories,[4,5] and computer simulations[6,7] show a smooth change from the mechanism of nucleation and growth to the mechanism of spinodal decomposition. These results thus suggest that the spinodal is a diffuse region; if not, the whole concept would lose its entire meaning.

In regards to the above, it is important to determine the range of validity of existing theories for the kinetics of decomposition. Another point of interest concerns the kinetics of coarsening of the decomposed structure. Lifshitz and Slyozov[8] derived a time exponent of $\frac{1}{3}$ in their theory of coarsening, while other theories predict a different time exponent. The scaling theory proposed by Lebowitz *et al.*[7] seems to hold for the later stages of decomposition. Up until now this theory has only been tested for a few cases. To test the theories mentioned above, a neutron scattering study was undertaken on a number of Cu-Ni-Fe alloys.

II. THEORY

A. Nucleation and growth

When an alloy is quenched from the stable region of the phase diagram into the metastable regime, the alloy will decompose when the amplitude of the concentration fluctuations is sufficiently large. First, small nuclei are formed which already have the composition of the final equilibrium phases. If these nuclei exceed a critical size they will grow by diffusion of the precipitating element.

A measure of the mean size of the clusters is the so-called radius of gyration R_G. For a homogeneous particle the radius of gyration is defined by

$$R_G^2=\frac{1}{V_P}\int_{V_P} r^2 d^3\vec{r}\,, \tag{2.1}$$

where V_P is the volume of the particle and $\vec{r}$ is a vector inside the particle with its origin in the center of gravity. The concept of the radius of gyration is applicable to particles of any shape.

B. Dynamical scaling of the structure function

Several authors[7,9,10] have investigated the scaling behavior of the time-dependent structure function during decomposition in the metastable and unstable region of the phase diagram. The scaling procedure is based on the assumption that, for late times after the quench, the mean "diameter" of the grains is much larger than the thermal correlation length and therefore the former is the relevant length scale for the description of the decomposition. We will use the scaling procedure as described by Lebowitz *et al.*[7] The function to be scaled is the function $S_1(\vec{\kappa},t)$, which is defined by

$$S_1(\vec{\kappa},t)=S(\vec{\kappa},t)-S_E(\vec{\kappa}) , \tag{2.2}$$

where $S(\vec{\kappa},t)$ is the structure function at a time t, $S_E(\vec{\kappa})$ is the structure function of the decomposed system, and $\vec{\kappa}$ is a wave vector. In the scaling procedure only the first moment κ_1 of $S_1(\vec{\kappa},t)$ is used, but in connection with the description of coarsening, which will be discussed later, the second moment κ_2 is also important. In general, the nth moment κ_n of the structure function is defined by

$$\kappa_n=\int_0^{\kappa_B}\kappa^n S_1(\vec{\kappa},t)d\vec{\kappa}\Big/\int_0^{\kappa_B}S_1(\vec{\kappa},t)d\vec{\kappa} , \tag{2.3}$$

where κ_B is some cutoff. The scaled function is defined by

$$F(x,t)\equiv\kappa_1^3(t)S_1(\vec{\kappa},t)\Big/\int_0^{\kappa_B}S_1(\vec{\kappa},t)d\vec{\kappa} \tag{2.4}$$

with

$$x\equiv\kappa/\kappa_1(t) . \tag{2.5}$$

Lebowitz *et al.*[7] found that, for their simulations for systems within the miscibility gap, $F(x,t)$ was, except for the early stages of the decomposition, independent of time $[F(x,t)=F(x)]$. The time-independent function $F(x)$ appeared to depend to some degree on the location of the quenched state inside the miscibility gap. When experimental data are used in the scaling procedure the structure function for the decomposed alloy is usually not measured because the equilibrium state cannot be attained in an experimentally accessible period of time and therefore $S(\vec{\kappa},t)$ is used instead of $S_1(\vec{\kappa},t)$.[11]

C. Coarsening

Lifshitz and Slyozov[8] gave a description for the process of coarsening in direct space (the growth of large grains of the new phase at the expense of smaller ones) for supersaturated systems close to the coexistence line. Coarsening is the mechanism that is assumed to be responsible for the later stages of the decomposition for a system of spherical grains, of which the mean radius R_m is small compared to the mean distance between them, where diffusion is assumed to be rate controlling. The time dependence of the mean radius of the spherical particles is given by[12]

$$R_m^3-R_0^3=kt , \tag{2.6}$$

where R_0 is the mean radius at time $t=0$ and k is a rate constant. When the particles are not spherical an appropriate mean particle size can be used instead of R_m for the evaluation of the data. The factor R_0^3 in Eq. (2.6) can be neglected except for the very early stages of the decomposition. Thus for longer annealing times, Eq. (2.6) can be approximated by

$$R_m=(kt)^{1/3} . \tag{2.7}$$

Although the theory of Lifshitz and Slyozov is, strictly speaking, only valid for a very small region inside the miscibility gap close to the coexistence line, Eq. (2.6) has also been successsfully used for the description of the decomposition of alloys which were quenched deeper into the miscibility gap.

Binder *et al.*[13] have derived another coarsening law based upon a consideration of the diffusion process on the atomic scale. The alloy was assumed to decompose in rather compact grains of almost pure components. Binder *et al.* predicted a much smaller exponent for t than Lifshitz and Slyozov, i.e.,

$$R_m=(kt)^{1/6} , \tag{2.8}$$

and they suggested that at first the coarsening can be described by Eq. (2.8), while for longer annealing times the Lifshitz-Slyozov theory gives the correct description of the coarsening [Eq. (2.7)]. Hence for longer annealing times, Eqs. (2.7) and (2.8) may be generalized to

$$R_m=(kt)^n . \tag{2.9}$$

To estimate the activation energy for coarsening (E_c), the rate constant k is assumed to be given by

$$k=k_0\exp(-E_c/RT_a) , \tag{2.10}$$

where k_0 is a constant, T_a is the annealing temperature, and R is the gas constant.

III. INTERPRETATION OF SCATTERING EXPERIMENTS

In this section we will discuss the predictions of the various theories for the scattering cross section in the small-scattering-vector ($\vec{\kappa}$) range, which is usually defined by[12]

$$0<|\vec{\kappa}|<\pi/d_a , \tag{3.1}$$

where d_a is the nearest-neighbor distance in the sample. For condensed matter this results in an upper limit of the small-scattering-vector range of $\kappa\cong 10\ \mathrm{nm}^{-1}$.

As mentioned in Sec. II, a measure of the mean size of the particles that are formed during decomposition is the radius of gyration. According to Guinier and Fournet,[14] the structure function can be approximated by a function of R_G (for small values of κR_G) as follows (the so-called Guinier approximation):

$$S(\vec{\kappa},t)=S(0)\exp[-\kappa^2R_G^2(t)/3] . \tag{3.2}$$

Strictly speaking, expression (3.2) is valid only for a single particle. It may, however, also be used for a system of particles when interference effects are negligible, viz., for dilute systems. For a spherical particle, for example, this approximation is valid for $\kappa R_G\leq 1.3$, while for a rod, $\kappa R_G\leq 0.7$.[14] For concentrated systems the effect of interparticle interference cannot be neglected, which results in the development of a peak for the structure function for $\kappa=\kappa_m$ ($\neq 0$). Yet the application of the Guinier approximation is still useful for $\kappa>\kappa_m$, as has recently been discussed by, e.g., Fratzl *et al.*[15] These authors state that cluster-interference effects are restricted to the small-κ region of the structure function. Although the meaning of the deduced Guinier radius is not well defined here, it turns out to be a good scaling parameter.

IV. EXPERIMENTAL TECHNIQUES

A. Sample preparation

The small-angle- and sideband-scattering intensities for alloys are proportional to the differences of the scattering factors of the elements in the alloy. Cu and Ni are neighbors in the Periodic Table. Consequently, the difference of the scattering lengths for x rays is very small $[(f_{Cu}-f_{Ni})/f_{Cu}\cong 0.03]$. The difference of the mean scattering lengths of the natural mixture of isotopes of Cu and Ni for thermal neutrons is much larger $[(b_{Cu}-b_{Ni})/b_{Cu}\cong 0.36]$ than for x rays and can even be increased fivefold $[(b_{Cu}-b_{Ni})/b_{Cu}\cong 1.78]$ by the use of the isotopes ^{62}Ni, which has a large negative scattering length for thermal neutrons $[b(^{62}\text{Ni})=-0.87\times 10^{-14}\text{m}]$ and ^{65}Cu, which has a large positive scattering length for thermal neutrons $[b(^{65}\text{Cu})=1.11\times 10^{-14}\text{m}]$. For the specimen preparation, Cu enriched in ^{65}Cu (99.7 at.%), Ni enriched in ^{62}Ni (98.0 at.%) and Fe (99.99% pure) of natural composition ($b_{Fe}=0.95\times 10^{-14}$ m) were used. The isotopes were purchased from Oak Ridge National Laboratory. Before melting, the mixture was reduced in a hydrogen flow at 1173 K. The material was melted in an Ar atmosphere containing 5 vol% H_2 in order to prevent evaporation of Cu and to increase the heat transfer (cooling rate) after melting. The ingots were cold-rolled and homogenized by annealing the polycrystalline specimens for one week at 1373 K in a quartz tube filled with Ar (5×10^4 Pa).

All of the specimens were annealed in a vertical furnace at 973 K, subsequently quenched in water, and the diffraction pattern of the quenched state was then determined. Subsequently, the specimens were annealed at the desired temperature for increasing periods of time. The experiments were performed at room temperature. A more detailed discussion of the sample preparation and heat treatments has been given by Vrijen.[16,17] The samples showed a pronounced texture, which turned out to influence the intensity of the Bragg peaks but had no effect on the intensity for small scattering angles. The composition of the alloys used for our investigation are shown in Fig. 1 together with the miscibility gap calculated by Hasebe and Nishizawa,[18] who used a subregular solution model to extrapolate experimental data obtained at higher temperatures.

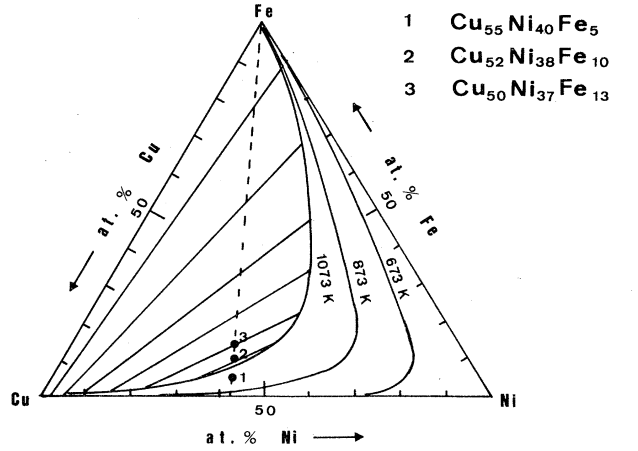

FIG. 1. Incoherent miscibility gap of the Cu-Ni-Fe system for $T=1073$, 873, and 673 K calculated by Hasebe and Nishizawa (Ref. 18). The composition of the Cu-Ni-Fe alloys used for the investigations described in this paper and a number of calculated tie-lines for $T=1073$ K are also indicated.

B. Measuring technique

The neutron scattering experiments were performed with a diffractometer with a one-dimensional position-sensitive detector 100 cm long and 2.5 cm in diameter at the reactor HFR (high-flux reactor) at Petten. A detailed description, together with the applied calibration and correction procedures, has been given elsewhere.[19]

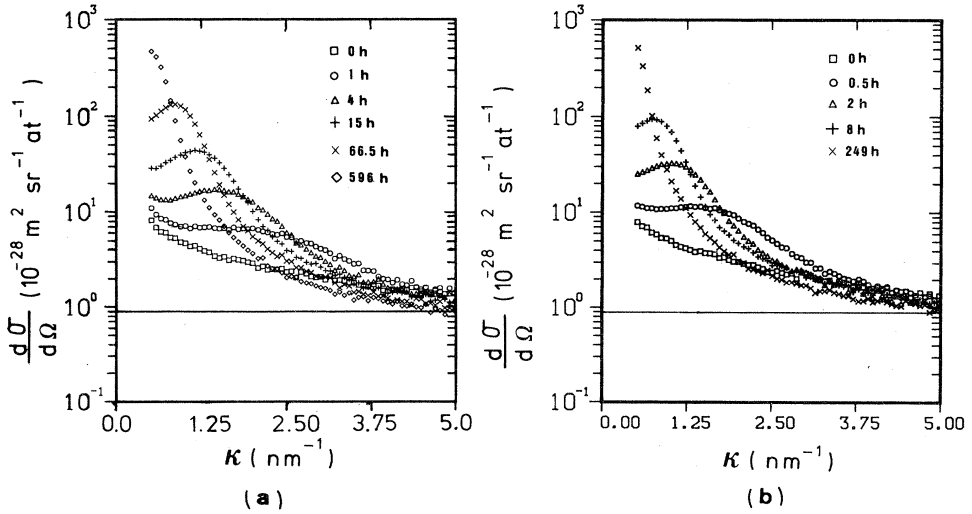

FIG. 2. Elastic neutron scattering cross section as a function of the scattering vector for different annealing times for a $Cu_{55}Ni_{40}Fe_5$ alloy annealed (after quenching from 973 K) at (a) 733 K and (b) 773 K. The solid line gives the neutron scattering cross section for the case in which the atoms are randomly distributed.

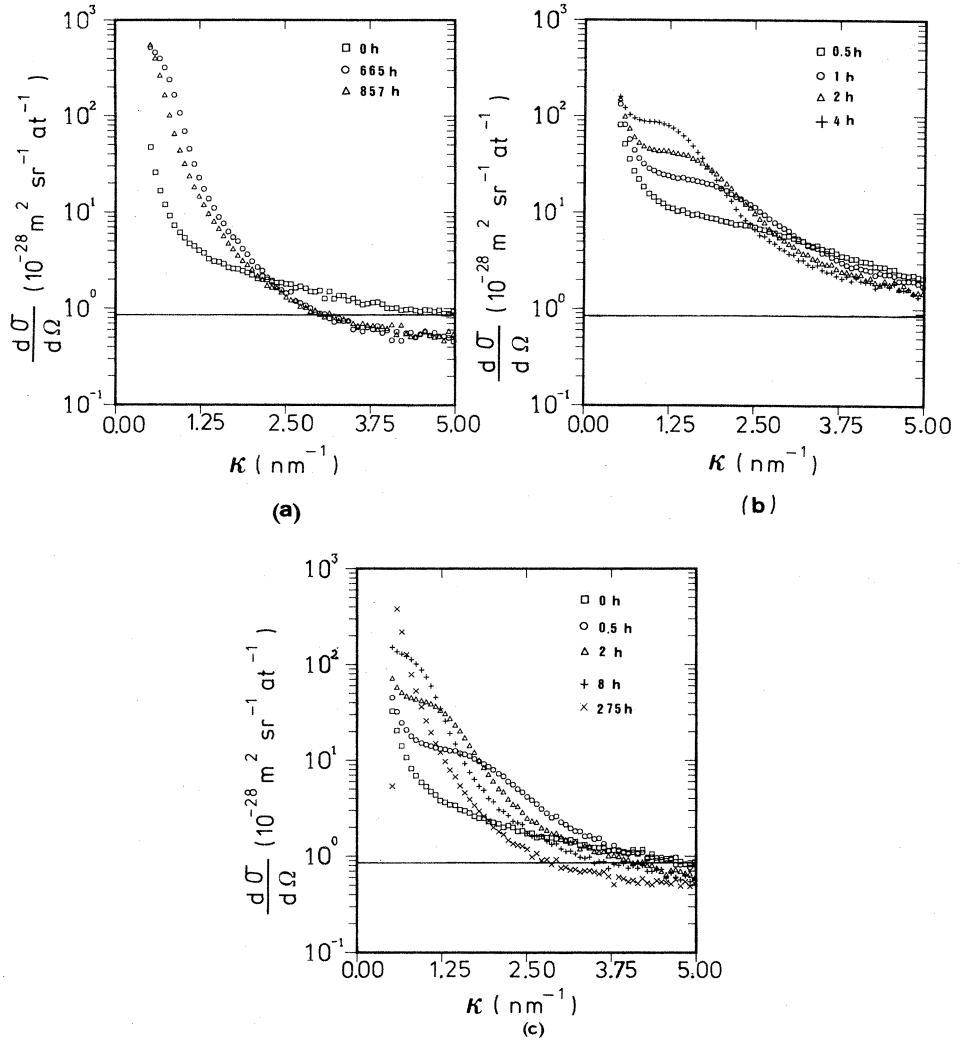

FIG. 3. Same as Fig. 2 for a $Cu_{52}Ni_{38}Fe_{10}$ alloy annealed at (a) 733 K, (b) 758 K and (c) 773 K.

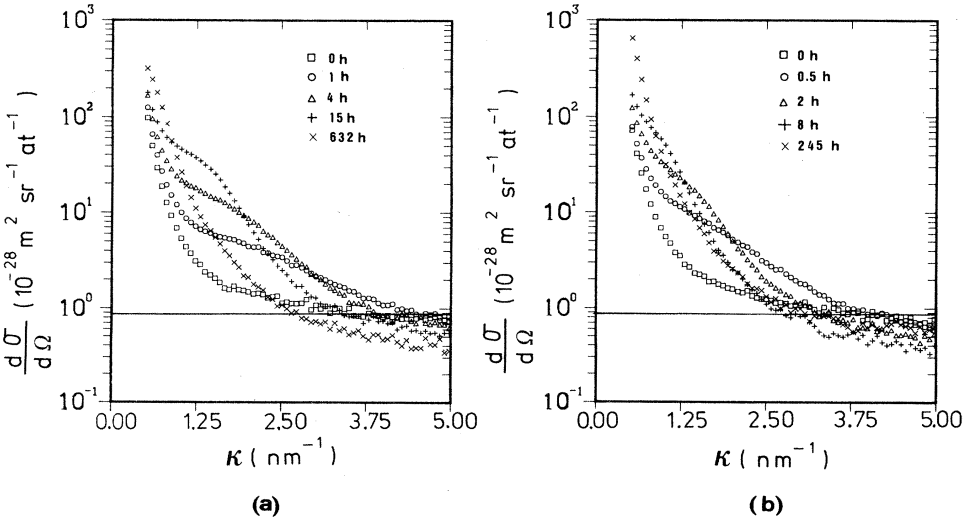

FIG. 4. Same as Fig. 2 for a $Cu_{50}Ni_{37}Fe_{13}$ alloy annealed at (a) 733 K and (b) 773 K.

V. EXPERIMENTAL RESULTS AND DATA ANALYSIS

A. Coarsening

The neutron scattering cross section was measured for different annealing times for three Cu-rich Cu-Ni-Fe alloys (see Figs. 2–4). The alloys $Cu_{55}Ni_{40}Fe_5$ and $Cu_{50}Ni_{37}Fe_{13}$ were annealed at 733 and 773 K. The $Cu_{52}Ni_{38}Fe_{10}$ alloy was annealed at 733 (only long annealing times), 758, and 773 K. It was verified by x-ray diffraction that these alloys did decompose at these annealing temperatures and that the $Cu_{52}Ni_{38}Fe_{10}$ and $Cu_{50}Ni_{37}Fe_{13}$ alloys already started to decompose at the quench temperature (973 K). However, we did not use higher quenching temperatures for these two alloys because we wanted to avoid the effect of quenched-in vacancies.

For the description of the coarsening process a number of parameters can be used, viz., the radius of gyration [Eq. (2.1)], the first and second moments of the structure function [Eq. (2.3)], or the mean wavelength of the composition modulations calculated from the position of the sidebands.

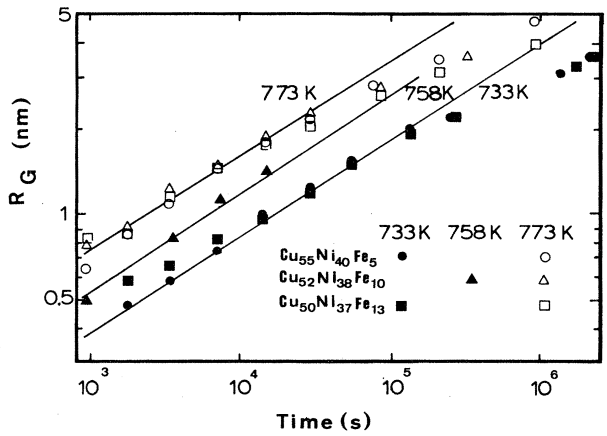

FIG. 5. Radius of gyration as a function of time for three Cu-Ni-Fe alloys.

First, we will discuss the time evolution of the radius of gyration, which can be deduced from the scattering function using Eq. (3.2). When the cube of the radius of gyra-

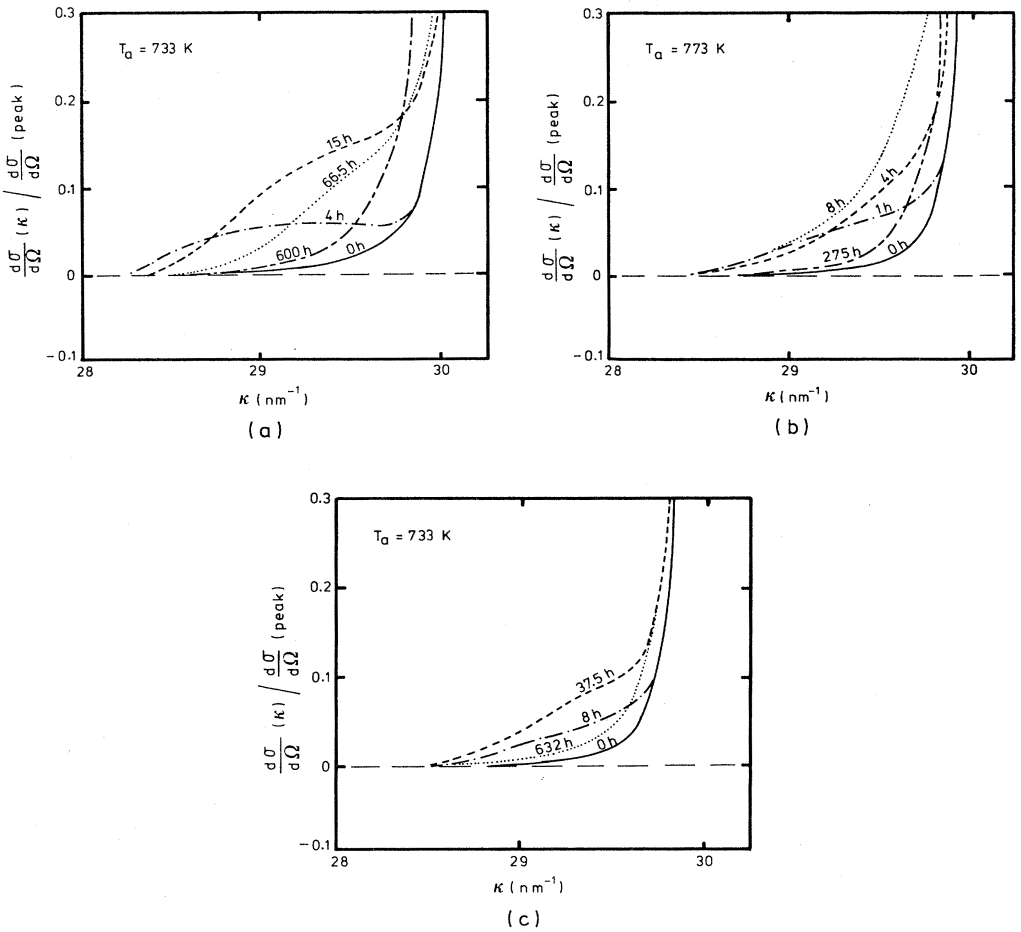

FIG. 6. Sideband intensity relative to the peak intensity near the (111) reflection for (a) $Cu_{55}Ni_{40}Fe_5$ and (c) $Cu_{50}Ni_{37}Fe_{13}$ alloys annealed at 733 K, and for a (b) $Cu_{52}Ni_{38}Fe_{10}$ alloy annealed at 773 K.

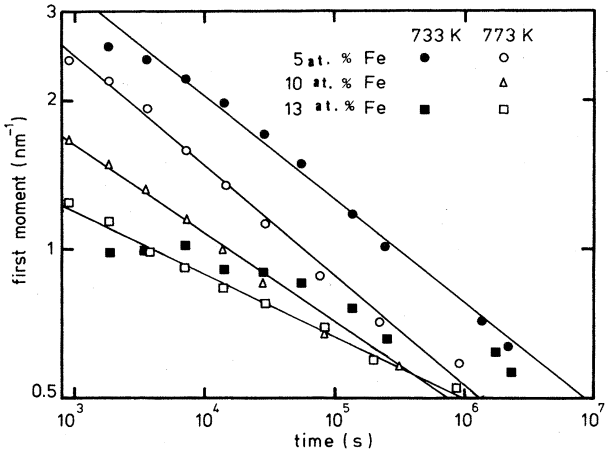

FIG. 7. First moment (κ_1) of the scattering function versus time for three Cu-Ni-Fe alloys.

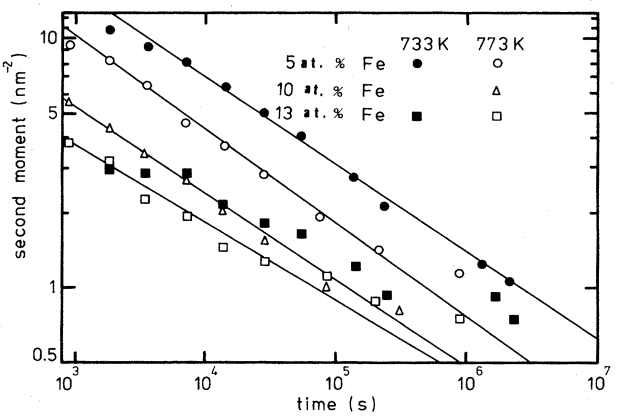

FIG. 8. Second moment (κ_2) of the scattering function versus time for three Cu-Ni-Fe alloys.

tion R_G is plotted versus time t and the resulting curves are extrapolated to $t=0$, the mean radius R_0 for the quenched state [see Eq. (2.6)] can be determined. The calculated R_0 values are very small and therefore it is justified to plot $\log R_G$ versus $\log t$ instead of R_G^3 versus t (see Fig. 5). As can be seen from this figure the time dependence of the radius of gyration (except for longer annealing times for which $R_G \geq 2$ nm) can be described by the Lifshitz-Slyozov theory ($n=1/3$, solid lines). For the later stages of decomposition the coarsening rate decreases.

In addition to the determination of the structure function for smaller values of the scattering vector we mea-

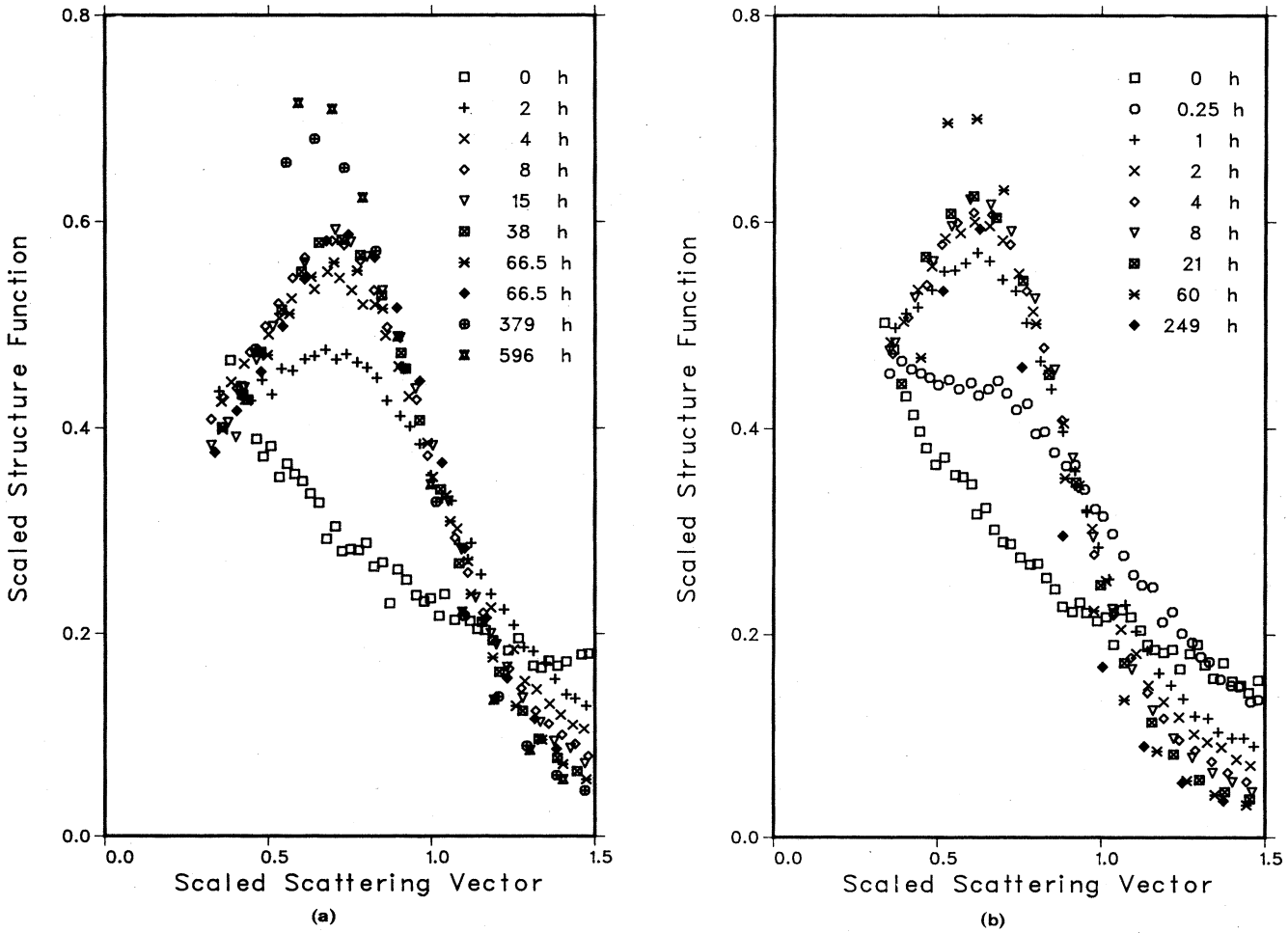

FIG. 9. Scaled function $F(x,t)$ for a $Cu_{55}Ni_{40}Fe_5$ alloy annealed at (a) 733 K and (b) 773 K.

TABLE I. Exponential values n_i used in Eq. (5.1) to describe the time dependence of coarsening.

Alloy	733 K		773 K	
	n_1	n_2	n_1	n_2
$Cu_{55}Ni_{40}Fe_5$	0.20	0.34	0.22	0.37
$Cu_{52}Ni_{38}Fe_{10}$			0.17	0.34
$Cu_{50}Ni_{37}Fe_{13}$			0.13	0.23

sured the neutron scattering cross section around the (111) and (200) reflections. The $Cu_{55}Ni_{40}Fe_5$, $Cu_{52}Ni_{38}Fe_{10}$, and $Cu_{50}Ni_{37}Fe_{13}$ alloys were annealed at 733 and 773 K, and at both temperatures sidebands appeared near the reflections. The scattering vector for the intensity maxima of the sidebands is related to the wavelength of the concentration modulation during decomposition, while the intensity of the sidebands is related to the amplitude of the concentration modulation. Owing to experimental circumstances we could measure only the sideband intensity on one side of the Bragg peak.

In Fig. 6 the time dependence of the (low-angle) sideband intensity near the (111) reflection is shown for $Cu_{55}Ni_{40}Fe_5$ and $Cu_{50}Ni_{37}Fe_{13}$ alloys annealed at 733 K and for a $Cu_{52}Ni_{38}Fe_{10}$ alloy annealed at 773 K. With increasing annealing time the sidebands move toward the main peak. No clear maximum in the sidebands could be detected, which might be due to the fact that it would develop too close to the Bragg reflections. Consequently, the mean wavelength of the composition modulation could not be reliably determined. However, the time dependence of the inverse of the mean wavelength is similar to the time dependence of the first moment of the structure function κ_1 (see the following).

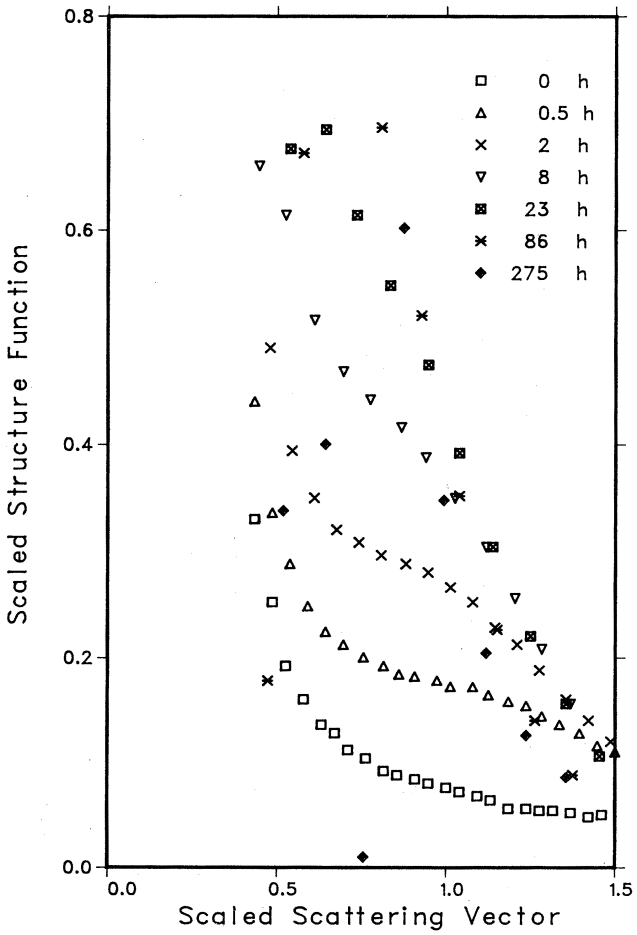

FIG. 10. Scaled function $F(x,t)$ for a $Cu_{52}Ni_{38}Fe_{10}$ alloy annealed at 773 K.

For the neutron scattering experiments described in this section we could only determine κ_m for the $Cu_{55}Ni_{40}Fe_5$ alloy for the longer annealing times at 733 and 773 K, while for the other alloys the position of the maximum of the scattered intensity could not be determined at all. The scattering curves of the other as-quenched alloys already showed pronounced small-angle scattering with probably a peak for $\kappa_m < 0.5$ nm^{-1}, which was the smallest value of the scattering vector that could be measured with our diffraction geometry. For that reason we used κ_1 and κ_2, which could be calculated for all cases, to investigate the coarsening. The mean diameter of the particles or, alternatively, the wavelength of the composition fluctuations, is proportional to κ_1^{-1}. Therefore, analogous to Eq. (2.9), we may write

$$\kappa_i^{-1} \propto t^{n_i} \quad (i=1,2) . \tag{5.1}$$

A plot of $\log\kappa_1$ (see Fig. 7) or $\log\kappa_2$ (Fig. 8) versus $\log t$ gave a reasonably straight line for all three alloys annealed at 773 K and for the $Cu_{55}Ni_{40}Fe_5$ alloy annealed at 733 K. However, for the $Cu_{52}Ni_{38}Fe_{10}$ alloy annealed at 758 K and the $Cu_{50}Ni_{37}Fe_{13}$ alloy annealed at 733 K $\log\kappa_1$ (or $\log\kappa_2$) and $\log t$ were not linearly related. The calculated values for n_i are given in Table I.

B. Dynamical scaling

Lebowitz *et al.*[7] showed that the structure functions obtained from computer simulations of the decomposition of a binary alloy show a scaling behavior after a certain transient period. We found that the structure function of a $Cu_{55}Ni_{40}Fe_5$ alloy (Fig. 2) could also be scaled (Fig. 9) using the relation [Eq. (2.4)] given by Lebowitz *et al.*[7] The structure function for the $Cu_{52}Ni_{38}Fe_{10}$ and $Cu_{50}Ni_{37}Fe_{13}$ alloys, however, could not be scaled using this equation (Figs. 10 and 11).

C. Long-range order

In the NiFe binary section of the Cu-Ni-Fe phase diagram, an ordered phase Ni_3Fe will form below $T=780$ K for compositions close to Ni_3Fe; this ordering also occurs (although at lower temperatures) when small amounts of Cu are added to the Ni_3Fe alloy.[20]

After each annealing step, we measured, in addition to the scattering cross section for small values of κ and the intensity of the sidebands, the scattering cross section for κ values near the (100) position. The diffraction pattern for the Cu-Ni-Fe alloys annealed at 773 K for about 250 h did not show any extra intensity at the (100) position. When these alloys were annealed (for 600—665 h) at 733

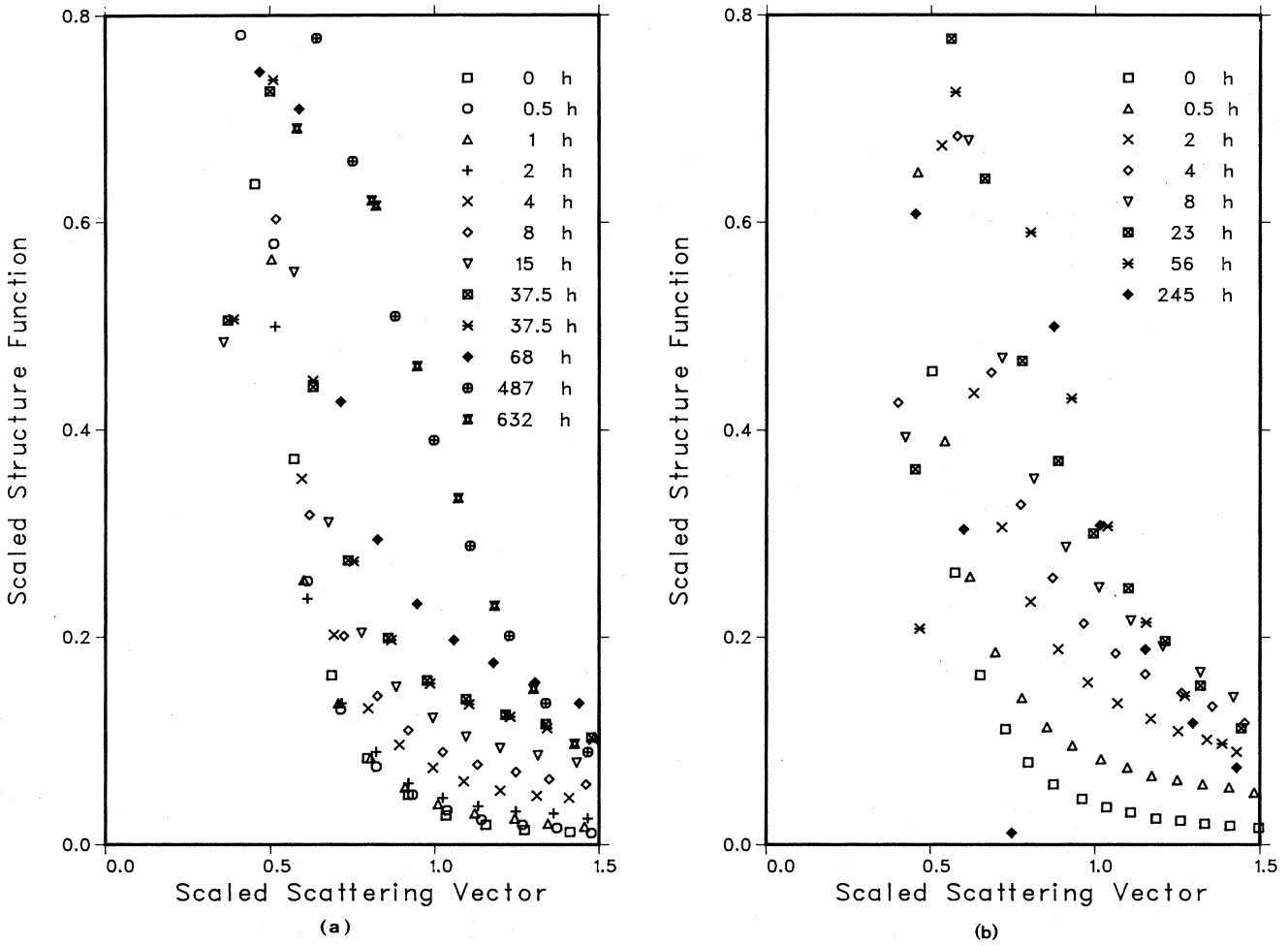

FIG. 11. Scaled function $F(x,t)$ for a $Cu_{50}Ni_{37}Fe_{13}$ alloy annealed at (a) 733 K and (b) 773 K.

K the diffraction pattern for the $Cu_{52}Ni_{38}Fe_{10}$ alloy did show a broad peak at the (100) position [Fig. 12(a)]. As a check we measured the diffraction pattern for the $Cu_{52}Ni_{38}Fe_{10}$ alloy after annealing for 860 h. The diffraction pattern showed a broad peak near the (100) and (110) positions [Fig. 12(b)]. We think that this is due to the formation of an ordered Ni_3Fe-type structure. For the composition of the NiFe phase in which the other two alloys decompose, the annealing temperature is either above the ordering temperature or no ordering occurs at all.

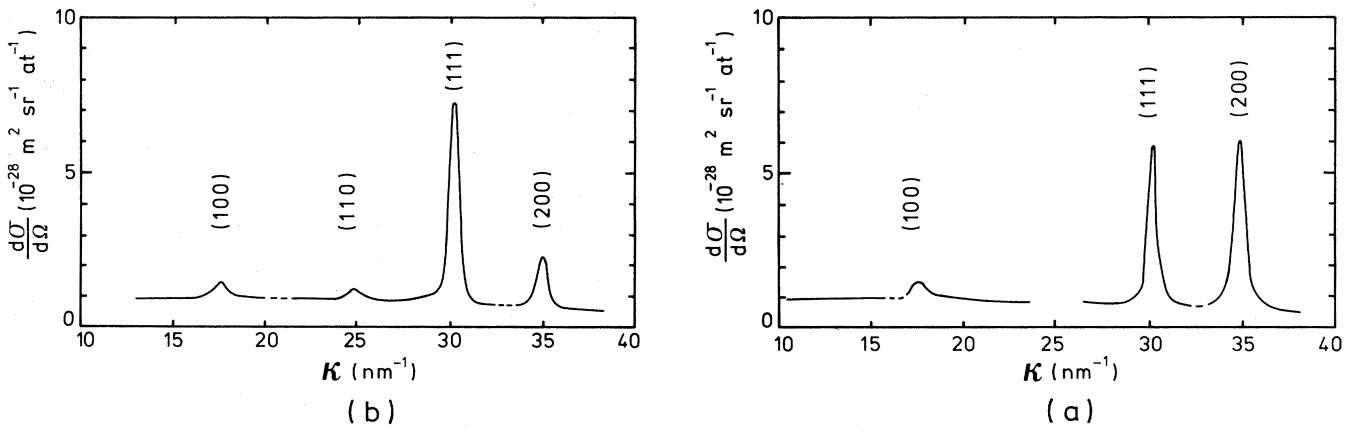

FIG. 12. Diffraction pattern for a $Cu_{52}Ni_{38}Fe_{10}$ alloy after annealing for (a) 665 h and (b) 857 h at 733 K, showing the (100) and (110) superlattice reflections.

VI. DISCUSSION AND CONCLUSIONS

We have already mentioned that the $Cu_{52}Ni_{38}Fe_{10}$ and $Cu_{50}Ni_{37}Fe_{13}$ alloys showed a certain amount of decomposition after quenching from 973 K, while the quenched $Cu_{55}Ni_{40}Fe_5$ alloy was still one phase. Annealing of the $Cu_{52}Ni_{38}Fe_{10}$ and $Cu_{50}Ni_{37}Fe_{13}$ alloys at a lower temperature than 973 K caused a change of the decomposition of the two phases, while the $Cu_{55}Ni_{40}Fe_5$ alloy started to decompose at the annealing temperatures (≤ 773 K). In the discussion of the results for the three Cu-Ni-Fe alloys this difference must be kept in mind.

First, we will treat the coarsening rate in terms of the radius of gyration. As can be seen from Fig. 5 the time evolution of the radius of gyration can, except for the longer annealing times, be described by the Lifshitz-Slyozov theory ($R_m \sim t^{1/3}$). For the longer annealing times the exponent of the time and thus the coarsening rate decreases ($n_i < 1/3$). The coarsening rates of $Cu_{52}Ni_{33}Fe_{15}$ (Ref. 21) and $Cu_{70}Ni_{21}Fe_9$ (Ref. 22) alloys were investigated with electron diffraction. The mean wavelength for these alloys as a function of time, which was calculated from the position of the sidebands near the Bragg peaks, could also be described with the Lifshitz-Slyozov theory ($n_i = 1/3$). However, Hillert *et al.*[2] found a different time dependence of the coarsening rate, namely, an exponent n_i which was between $\frac{1}{4}$ and $\frac{1}{5}$. In the present investigation we could determine the maximum of the observed sidebands only in the very early stages, even though these sidebands were present at all annealing temperatures for the three Cu-Ni-Fe alloys. Consequently, no quantitative conclusions about coarsening can be drawn from these data. We want to point out, however, that when null alloys (zero Bragg scattering) are used, very large satellites can be observed. In those cases, e.g., very useful information about the wavelength and the orientation of the composition modulation can be obtained.[23]

Another measure for the size of the nuclei in the alloys during the decomposition is given by the first moment (κ_1) of the scattering function. The time dependence of κ_1 could not be described by the Lifshitz-Slyozov theory

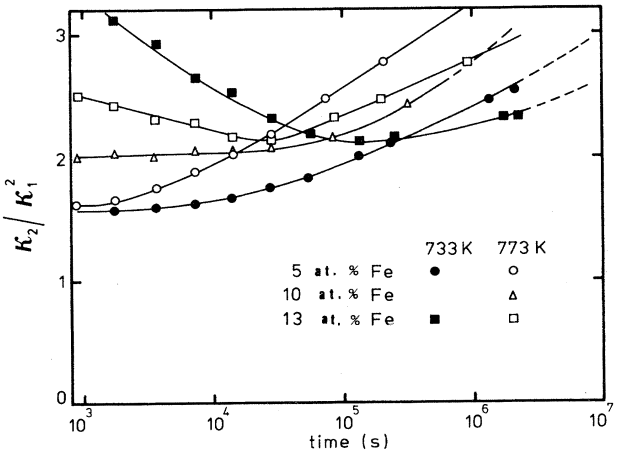

FIG. 13. Time dependence of κ_2/κ_1^2 for three Cu-Ni-Fe alloys. Lines are a guide for the eye.

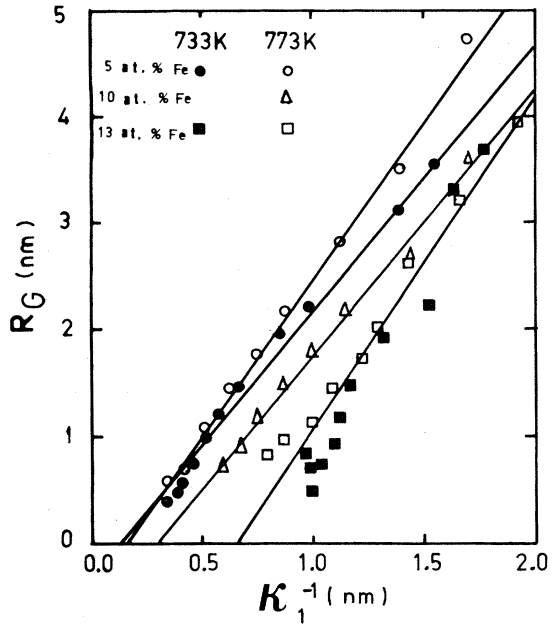

FIG. 14. Radius of gyration (R_G) versus the inverse of the first moment of the scattering function (κ_1^{-1}).

($n = 1/3$). When we move deeper into the miscibility gap, e.g., by adding more Fe or annealing at lower temperature, the values for n_i decrease; this effect was also observed for computer simulations.[7] Thus, close to the coexistence line the coarsening can be described by the Lifshitz-Slyozov theory, whereas when we move deeper into the miscibility gap the coarsening rate decreases. The first moment of the scattering function [Eq. (2.3)] is used in the dynamical scaling procedure described and tested for computer simulations by Lebowitz *et al.*[7] The second moment was also calculated for the computer simuations by Lebowitz *et al.* and it appeared that κ_2 divided by κ_1^2 was independent of the annealing time. In Fig. 13 the time dependence of κ_2/κ_1^2 is plotted for the alloys investigated. The scattering curves for the $Cu_{52}Ni_{38}Fe_{10}$ and $Cu_{50}Ni_{37}Fe_{13}$ alloys (decomposed) show a steep increase of the intensity for small κ values. Since it was not possible to measure the neutron scattering cross section for $\kappa < 0.5$ nm^{-1} with our neutron spectrometer we could not determine the peak position of these scattering curves. Consequently, the calculated values for κ_1 and κ_2 are also too high. This might explain our observation that the calculated value for κ_2/κ_1^2 is time dependent, contrary to results of computer simulations[7] and experiments on Al-Zn alloys.[11] On the other hand, the physical meaning of κ_2/κ_1^2 is not at all clear and might well be accidental.

The radius of gyration and the first moment of the scattering function are both a measure for the particle size. Consequently, a plot of R_G versus κ_1^{-1} should give a straight line (Fig. 14).

However, a comparison of Figs. 5 and 7 suggests that the Guinier radius gives a better description of the particle size than κ_1. This point of view is supported by a recent comparison of cluster sizes and densities obtained from

computer simulations and the ones obtained by the Guinier method from the structure function.[15]

The activation energy for the coarsening process (diffusion controlled) can be calculated from the temperature dependence of the rate constant k [see Eq. (2.10)]. The rate constant was calculated from the time dependence of the radius of gyration (Fig. 6). We found, for the activation energy, $E_c = 230$ kJ mol^{-1}, which shows good agreement with the value calculated by Butler and Thomas[21] ($E_c = 200$ kJ mol^{-1}). Hillert *et al.*,[2] who included the effect of the temperature dependence of the interfacial energy, and Daniel,[24] found $E_c = 275$ kJ mol^{-1}. For a $Cu_{50}Ni_{50}$ alloy the activation energy for self-diffusion for Cu into the Cu-Ni alloy, which is smaller than the activation energy for self-diffusion of Ni into the Cu-Ni alloy, is approximately 255 kJ mol^{-1}.[25]

The scattering function for the $Cu_{55}Ni_{40}Fe_5$ alloy shows, after a transient time, a scaling behavior. That the scattering functions for the $Cu_{52}Ni_{38}Fe_{10}$ and $Cu_{50}Ni_{37}Fe_{13}$ alloys do not show scaling behavior could be caused by the fact that these alloys were, to a certain extent, already decomposed after quenching. Moreover, the resolution in the small-κ region of the applied spectrometer was too poor to measure the maxima in the structure function of the latter two alloys in the decomposed state. These two facts make it impossible to be as conclusive as we hoped to be with respect to scaling. The observation of superlattice peaks, which can be ascribed to an ordered $L1_2$ phase (Ni_3Fe with a small amount of Cu), is in good agreement with a Cu-Ni-Fe phase diagram[26] calculated with the cluster-variation method.

We now summarize the results of the investigation described in this paper. The structure function for a ternary (Cu-Ni-Fe) alloy turned out to show the same scaling behavior as the structure function for binary alloys.[7,11] Since the radius of gyration and the first moment of the structure function are linearly related, these parameters appear to be a measure of the same effect. For the early stages of decomposition, the coarsening could be described with the Lifshitz-Slyozov theory, while for longer annealing times the coarsening rate decreased.

ACKNOWLEDGMENTS

We gratefully acknowledge Mrs. A. D. M. Brandt—van Rede and Mr. A. Bontenbal for their technical assistance in the neutron scattering experiments at Petten, Mr. Th. Klinkhamer for his cooperation in preparing the specimens, and Dr. Ir. Th. H. de Keijser, Ing. N. M. van der Pers, and Mr. H. D. F. Meijer (Laboratory of Metallurgy, Delft University of Technology) for the texture analysis and for the performance of the x-ray diffraction experiments. The Stichting Fundamenteel Onderzoek der Materie (FOM) sponsored this work with a grant for the isotopes.

[1] *The Scientific Papers of J. Williard Gibbs* (Dover, New York, 1961), p. 105.
[2] M. Hillert, M. Cohen, and B. L. Averbach, Acta Metall. **9**, 536 (1961).
[3] V. Gerolt and G. Kostorz, J. Appl. Crystallogr. **11**, 376 (1978).
[4] K. Binder, C. Billotet, and P. Mirold, Z. Phys. B **30**, 183 (1978).
[5] J. S. Langer, M. Bar-on, and H. D. Miller, Phys. Rev. A **11**, 1417 (1975).
[6] A. Sur, J. L. Lebowitz, J. Marro, and M. H. Kalos, Phys. Rev. B **15**, 3014 (1977).
[7] J. L. Lebowitz, J. Marro, and M. H. Kalos, Acta Metall. **30**, 297 (1982).
[8] I. M. Lifshitz and V. V. Slyozov, J. Phys. Chem. Solids **19**, 35 (1961).
[9] J. Marro, J. L. Lebowitz, and M. H. Kalos, Phys. Rev. Lett. **43**, 282 (1979).
[10] H. Furukawa, Phys. Rev. Lett. **43**, 136 (1979).
[11] M. Hennion, D. Ronzaud, and P. Guyot, Acta Metall. **30**, 599 (1982).
[12] V. Gerold and G. Kostorz, J. Appl. Crystallogr. **11**, 376 (1978).
[13] K. Binder, M. H. Kalos, J. L. Lebowitz, and J. Marro, Adv. Colloid Interface Sci. **10**, 173 (1979).
[14] A. Guinier and G. Fournet, *Small-Angle Scattering of X-Rays* (Wiley, New York, 1955).
[15] P. Fratzl, J. L. Lebowitz, J. Marro, and M. H. Kalos, Acta Metall. **31**, 1849 (1983).
[16] J. Vrijen, Doctor's thesis, Rijksuniversiteit Utrecht, 1977; Netherlands Energy Research Foundation (ECN), Petten (N.H.), Report No. ECN-31, 1977 (unpublished) (available on request).
[17] J. Vrijen, J. Aalders, C. van Dijk, and S. Radelaar, Phys. Rev. B **22**, 1503 (1980).
[18] M. Hasebe and T. Nishizawa, in *Applications of Phase Diagrams in Metallurgy and Ceramics,* Natl. Bur. Stand. Spec. Publ. No. 496, edited by G. C. Carter (U. S. GPO, Washington, D.C., 1978), p. 91.
[19] T. J. A. Aalders, Doctor's thesis, Rijksuniversiteit Utrecht, 1982; Netherlands Energy Research Foundation (ECN), Petten (N.H.), Report No. ECN-118, 1982 (unpublished) (available on request).
[20] V. I. Gomankov, I. M. Puzey, and Ye.I. Mal'tsev, Fiz. Met. Metalloved. **30**, 220 (1970) [Phys. Met. Metallogr. (U.S.S.R.) **30**, 237 (1970)].
[21] E. P. Butler and G. Thomas, Acta Metall. **18**, 347 (1970).
[22] R. J. Livak and G. Thomas, Acta Metall. **19**, 497 (1971).
[23] J. Aalders, C. van Dijk, and S. Radelaar, in On the Early Stages of Decomposition of Alloys, Proceedings of a conference, St. Andreasburg, Harz, 1983 (to be published) [Acta Metall.].
[24] V. Daniel, Proc. R. Soc. London, Ser. A **192**, 575 (1947).
[25] K. Monma, H. Suto, and H. Oikawa, J. Jpn. Inst. Met. **28**, 192 (1964).
[26] H. Yamauchi and S. Radelaar (unpublished).